COMMUNICATION

Novel Electric Double-Layer Capacitor with a Coaxial Fiber Structure

*Xuli Chen, Longbin Qiu, Jing Ren, Guozhen Guan, Huijuan Lin, Zhitao Zhang, Peining Chen, Yonggang Wang, and Huisheng Peng**

Portable and foldable electronic devices had been shown to be highly desired in the current life and further dominate the future life.[1–4] To this end, it becomes critically important to develop matchable energy storage systems such as electric double-layer capacitors (EDLCs) to power them. The EDLCs should be lightweight, flexible and stretchable, and could be easily integrated with high performances.[5–8] However, the available EDLCs typically appeared in a heavy and rigid plate which could not meet the above requirements.[9–11] Recently, some attempts were made to explore lightweight and flexible EDLCs in a wire format by twisting two fiber electrodes together.[12,13] Compared with the conventional planar structure, the wire-shaped EDLC could be woven into electronic clothes by the well-developed textile technology and show promising applications in a wide variety of fields. However, the high contact resistance between two twisted fiber electrodes has largely decreased the energy storage capability. In addition, they are not stretchable in the straight wire state, so the resulting electronic textiles based on the wire-shaped EDLC will break during the use.

Due to the remarkable mechanical, electrical, and thermal properties, carbon nanotubes (CNTs) have been widely studied as electrode materials to fabricate EDLCs.[14–16] CNTs could be used either as a conductive agent or for an electrode material. In addition, all CNT-based capacitors have been also realized mainly on the basis of liquid electrolytes such as aqueous KOH or H_2SO_4 solution and organic acetonitrile solution, although both of them exhibited relatively low specific capacitances, e.g., 10 F cm^{-3} and 20–40 F g^{-1} (with energy density of 69.4 Wh kg^{-1} and power density of 43.3 kW kg^{-1}), respectively.[17–19] In addition, complex fabrication processes are required to seal such capacitors with liquid electrolytes. To this end, several attempts are recently made to introduce organic electrolytes and ionic liquids to produce solid capacitors with specific capacitances over 20 F g^{-1}.[20,21] For the above liquid and solid electrolyte-based capacitors, they appeared in a heavy planar format. In particular, there remains a common and big challenge, i.e., CNTs are randomly aggregated in the active or electrode layer, which has largely limited their performance as the charges have to cross a lot of boundaries in the aggregated CNT networks. In other words, the excellent physical properties of individual CNTs, particularly, extraordinary electrical properties, had not been effectively demonstrated at their bulk materials. Recently, CNTs had been assembled into continuous fibers and sheets by a dry spinning process or wet spinning process.[22–24] For both fibers and sheets, CNTs were highly aligned to extend their excellent properties such as high mechanical strength and electrical conductivity from the nanometer to macroscopic scale. These aligned CNT materials shed light on the high-performance EDLCs.

In this communication, a novel family of coaxial EDLC fibers had been designed and produced from the aligned CNT fiber and sheet, which functioned as two electrodes with a polymer gel sandwiched between them. The unique coaxial structure had decreased the contact resistance between the two electrodes with a maximum discharge capacitance of 59 F g^{-1} (32.09 F cm^{-3} or 29 μF cm^{-1} or 8.66 mF cm^{-2}), much higher than 4.5 F g^{-1} of the EDLC by twisting two CNT fibers together. These EDLC fibers exhibit energy densities up to 1.88 Wh kg^{-1} and power densities up to 755.9 W kg^{-1}. In addition, they are flexible and stretchable, and can be easily scaled up with high efficiency and low cost.

Both CNT fibers and sheets were dry-spun from CNT arrays that had been synthesized by a chemical vapor deposition method. By varying the width of the starting CNT ribbon during the spinning process, the CNT fiber can be controlled from 6 to 40 μm in diameter and the CNT sheet can be controlled from 0.1 to 4 cm in width. Due to the highly aligned structure of CNTs, the resulting fiber and sheet showed electrical conductivity on the level of (10^2–10^3) S cm^{-1} and tensile strength on the order of (10^2–10^3) MPa. There were appropriately a million CNTs in the cross section of the fiber or sheet with distances among neighboring CNTs of several to tens of nanometers, so a high surface area on the level of 10^2 m^2 g^{-1} and low density of 0.54 g cm^{-3} had been obtained. The second phase such as a gel electrolyte containing poly(vinyl alcohol) (PVA) and H_3PO_4 could be effectively incorporated into the CNT fiber and sheet. The gel electrolyte functioned not only as a conducting media but supporting material to enable the stretchability of the EDLC fiber.

X. Chen, L. Qiu, J. Ren, G. Guan, H. Lin, Z. Zhang, P. Chen, Prof. H. Peng
State Key Laboratory of Molecular Engineering of Polymers
Department of Macromolecular Science and Laboratory of Advanced Materials
Fudan University
Shanghai, 200438, China
E-mail: penghs@fudan.edu.cn
Prof. Y. Wang
Department of Chemistry, and Shanghai Key Laboratory of Molecular Catalysis and Innovative Materials
Institute of New Energy
Fudan University
Shanghai, 200438, China.

DOI: 10.1002/adma.201301519

© 2013 WILEY-VCH Verlag GmbH & Co. KGaA, Weinheim

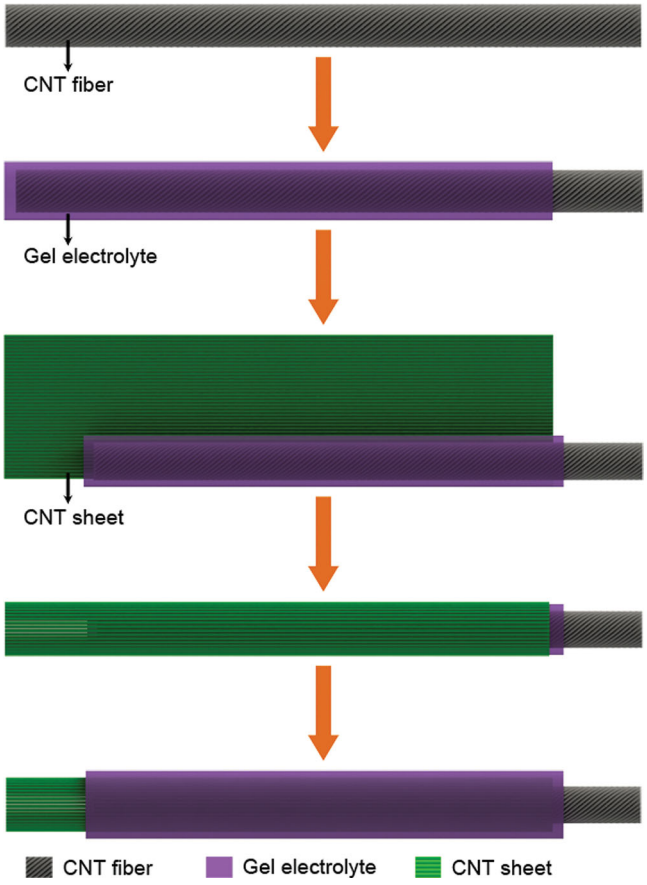

Figure 1. Schematic illustration to the fabrication of a coaxial EDLC fiber bases on CNT fiber and sheet as two electrodes.

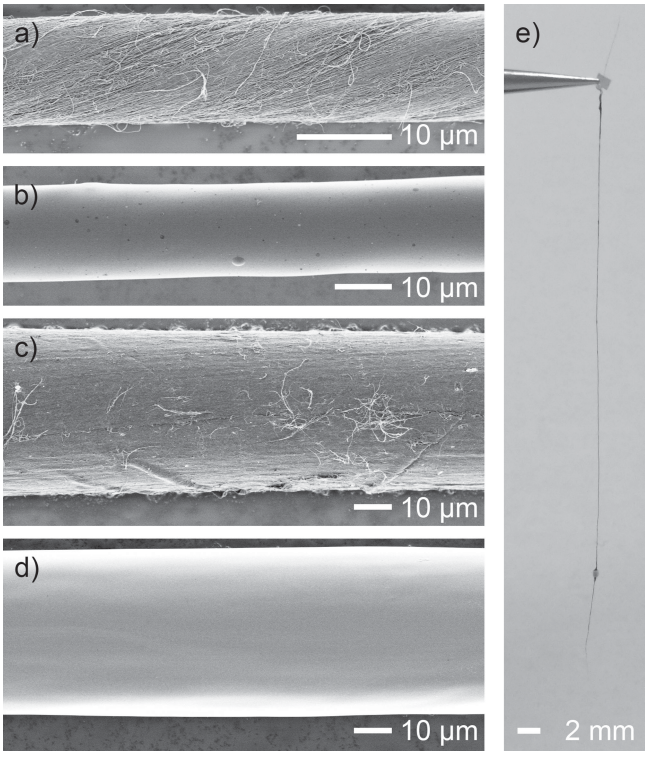

Figure 2. Scanning electron microscopy (SEM) images of a) a CNT fiber; b) CNT fiber incorporated with PVA/H_3PO_4 electrolyte, c) CNT sheet covered on (b); d) Dipping treatment of (c) with PVA/H_3PO_4 electrolyte; e) Photograph of a coaxial EDLC fiber.

Figure 1 has schematically shown the detailed fabrication process of a typical EDLC fiber. Firstly, a CNT fiber was dipped into the PVA/H_3PO_4 electrolyte which could be both infiltrated into the fiber and coated on the surface. A CNT sheet was then scrolled on the resulting fiber to produce the desired EDLC fiber. To improve the electrochemical performance, the fiber device was further dipped into the same gel electrolyte again to make sure that all CNTs in the sheet had been embedded in the electrolyte. **Figure 2** shows scanning electronic microscopy (SEM) images and a photograph during the fabrication of a EDLC fiber. The CNT fiber with uniform diameter of 11.5 μm had been typically used as the core electrode (Figure 2a). As previously mentioned, the building CNTs were highly aligned with each other. After incorporation of the gel electrolyte, a composite fiber with increased diameter of appropriately 17 μm had been obtained (Figure 2b and Figure S1, Supporting Information). As the infiltration of the second phase, which was mainly filled with the voids among aligned CNTs, did not obviously change the fiber diameter, a uniform electrolyte layer with thickness of 2.75 μm was formed on the surface of the CNT fiber. A thin CNT sheet was then scrolled outside (Figure S2, Supporting Information), and the derived fiber exhibited increased diameter of 43 μm as the CNT sheet was loosely attached on the surface (Figure 2c). After the further dipping treatment in the same electrolyte, the EDLC fiber remained almost unchanged in diameter (Figure 2d), and a typical photograph was also shown in Figure 2e.

The structure of the EDLC fiber is schematically shown in **Figure 3**a. To verify the coaxial structure, the cross section of the EDLC fiber was further analyzed by SEM (Figure 3b). The breaking section of the fiber device was produced by the treatment of liquid nitrogen. To obtain the cross-section with high quality, here the EDLC fiber had been coated with a thicker layer of gel electrolyte. Two concentric cycles can be clearly observed from the cross section with the inner one as the surface part of CNT fiber and the outer one as CNT sheet. Under higher magnifications marked by the top and bottom boxes, it was found that CNTs had been maintained to be highly aligned in both sheet and fiber parts, and the gel electrolyte was filled among them (Figure S3,S4, Supporting Information).

Figure 4a shows a typical galvanostatic charge–discharge curve of the EDLC fiber between 0.005 and 1 V at a current of 10^{-7} A. The symmetric triangle shapes indicate that the EDLC fiber belongs to a EDLC with the highest Coulomb efficiency of 0.94. No obvious voltage spurts had been found at the beginning period in both charge and discharge processes. In other words, the EDLC fiber had a low internal resistance, which further indicated the low resistances of and between the two electrodes due to the unique coaxial structure. Therefore, both positive and negative ions have shared short transport

© 2013 WILEY-VCH Verlag GmbH & Co. KGaA, Weinheim

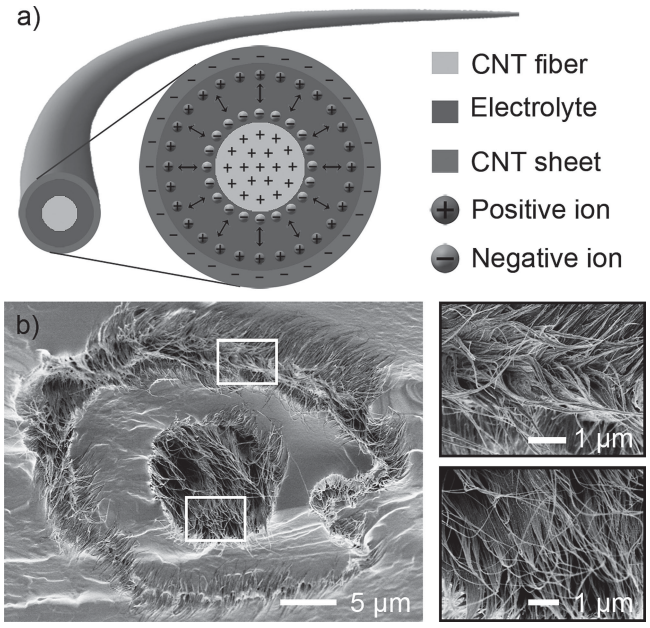

Figure 3. a) Schematic illustration to both the cross-sectional structure and mechanism for the high electrochemical property of the coaxial EDLC fiber. The electropositive CNT fiber and electronegative CNT sheet functioned as the positive and negative electrodes, respectively; b) SEM images at low (left image) and high (right images) magnifications for a cross section. The right images correspond to the left rectangle-labeled areas.

routes between the two electrodes during the charging and discharging processes, which favored a high electrochemical performance (Figure 3a). Figure 4b has further compared specific capacitances of the EDLC fiber with increasing electric currents of 1.00×10^{-7}, 2.00×10^{-7}, and 5.00×10^{-7} to 1.00×10^{-6} A. With the increasing current, the Coulomb efficiencies had been increased to appropriately 100%, and the specific capacitance had been maintained to be 88.40%. To investigate the stability of the EDLC fiber, a cyclic charge–discharge characterization was carried out (Figure 4c), and no obvious decrease in the capacitance had been found after 11 000 cycles. Figure 4d further shows cyclic voltammograms with increasing scan rates of 50, 200, 500, to 1000 mV s^{-1}. The rectangular shapes also indicate a double layer capacitor,[25] which agrees with Figure 4a. In addition, the rectangular shapes had been well maintained with the increasing scan rate, which has also verified a low internal resistance of the EDLC fiber and high performance during the rapid charge-discharge process. To further study the electrochemical performance, electrochemical impedance spectroscopy (EIS) was used to compare the coaxial and twisted structures (Figure 4e). Obviously, the coaxial structure shows a lower internal resistance, which is also verified by Galvanostatic charge–discharge curves in Figure 4f.

The mass ratio between CNT fiber and sheet was found to be critical for a high performance of the EDLC fiber, and an optimal value occurred at appropriately 1/1. For instance, when the mass ratio was decreased from 1/1 to 1/3, the specific capacitance had been reduced by appropriately 25%. The optimal mass ratio can be also theoretically concluded by the following calculation. For the two electrodes both based on aligned CNTs, the capacitance (C) is proportional to the mass (m), so $C_1 = nC_2$ as $m_1 = nm_2$, where n is constant while 1 and 2 stand for the CNT sheet and fiber electrodes, respectively. If C is used for the total capacitance of this EDLC where the two electrodes are connected in series, the relationship between C and C_1 and C_2 can be expressed below.

$$\frac{1}{C} = \frac{1}{C_1} + \frac{1}{C_2} \tag{1}$$

According to the definition of the specific capacitance (C_s),

$$C_s = \frac{C}{m} \tag{2}$$

Therefore,

$$C_{s1} = \frac{C_1}{m_1} \text{ and } C_{s2} = \frac{C_2}{m_2} \tag{3}$$

At the same time,

$$m = m_1 + m_2 \tag{4}$$

Based on the above four equations, it is found that

$$C_{s1} \equiv C_{s2} = \left(1 + \frac{1}{n}\right)\frac{C}{m_2} = \frac{(n+1)^2}{n} C_s \tag{5}$$

Finally,

$$C_s = \frac{n}{(n+1)^2} C_{s1} \tag{6}$$

The maximum C_s value is produced when $\frac{d\left[\frac{n}{(n+1)^2}\right]}{dn} = 0$, i.e., $1 - n = 0$. Obviously, $n = 1$ so the mass ratio between the two electrodes should be 1/1.

The EDLC fibers were flexible, and no obvious changes in structure had been detected by SEM under bending (Figure S5). As a result, there were almost no decrease in specific capacitance for them under bending in an angle range from 0 to 180° or a curvature range between 0 and 31.25 cm^{-1} (**Figure 5**a and 5b). The specific capacitance has been maintained by 97.2% after bending at 180° for over 100 cycles (Figure S6, Supporting Information). In addition, they were also stretchable. Figure 5c shows the dependence of the specific capacitance on the strain in a stretching and releasing cycle. The specific capacitance is slightly decreased with the increasing strain but can be fully reverted. Figure 5d further shows that the specific capacitance can be maintained to be 90.8, 84.6, and 81.6% after being stretched by 10% for 25, 50, and 75 cycles, respectively. The EDLC fiber was stretchable as the two flexible electrodes of CNT fiber and sheet were curved in and stabilized by the stretchable gel electrolyte.[23,26] The stretched degree of the EDLC fiber can be controlled by the curved degree of the CNT electrodes, and no breaking occurred before they are stretched to the linear structure (Figure S7, Supporting Information). A maximal strain of 100% has been currently achieved.

The increased capacitance at the first stretching process is explained by the fact that two electrodes were more efficiently contacted with the electrolyte when they were stretched. With the increasing stretching cycle, some CNTs in the two electrodes may be slipped with each other, and the internal resistance of the EDLC was slightly and gradually increased by comparing

© 2013 WILEY-VCH Verlag GmbH & Co. KGaA, Weinheim

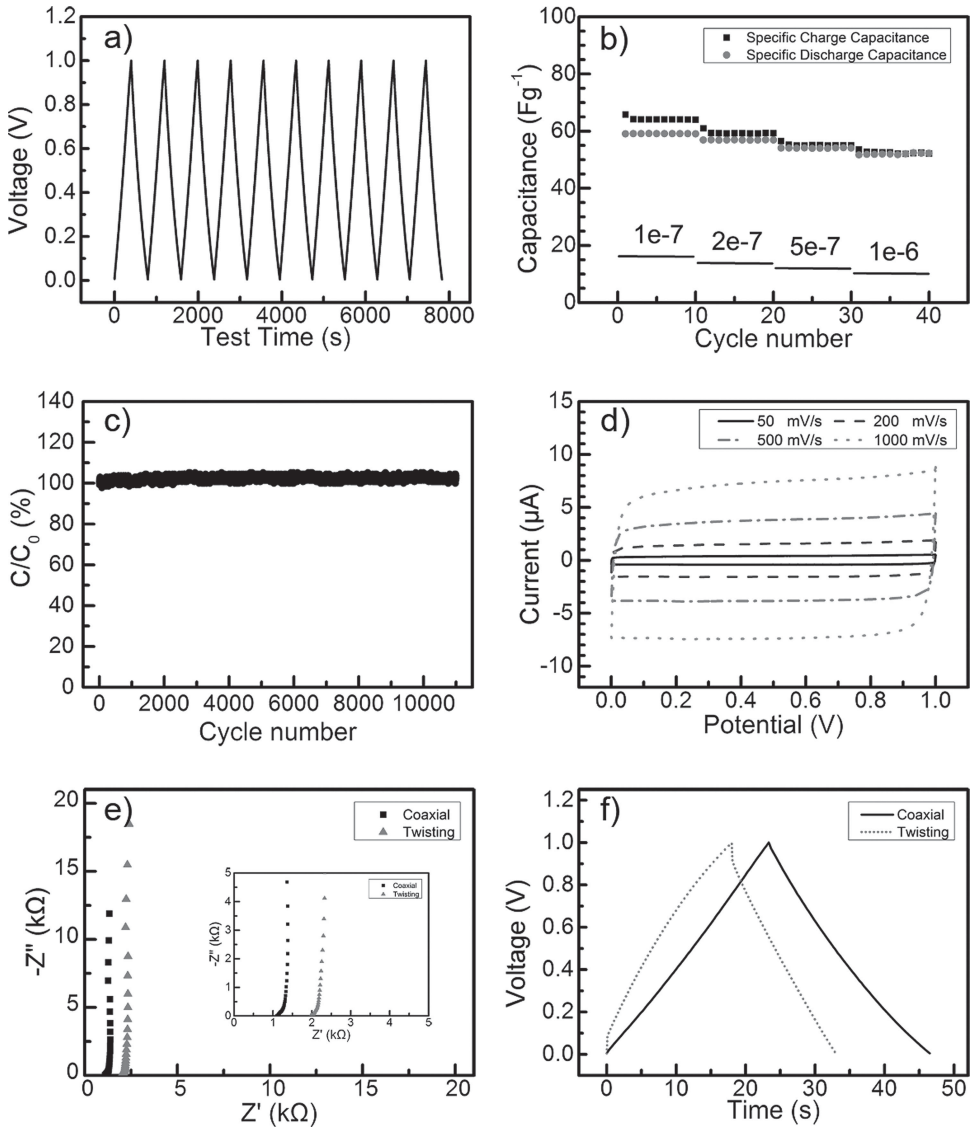

Figure 4. Electrochemical characterization of the EDLC fiber; a) Typical Galvanostatic charge-discharge profile at a current of 1.00×10^{-7} A. b) Cycle performance with the increasing electric current; c) Dependence of capacitance on cycle number at a current of 1.00×10^{-5} A. d) *I–V* curves with the increasing scan rate; e) Nyquist plots of EDLCs with both coaxial (square dots) and twisted (triangular dots) structures; f) Galvanostatic charge-discharge curves for coaxial (solid line) and twisted (dotted line) EDLCs at the same current of 1 μA.

the voltage spurt part (Figure S8, Supporting Information). The voltage spurt at the beginning charge and discharge processes became slightly increased with the increased stretching cycle. More efforts are needed to improve the interaction among CNTs by increasing the CNT length which improves entanglements of CNTs.

It should be noted that for the twisted wire-shaped EDLCs, the two fiber electrodes would be easily separated from each other during the bending, and the EDLCs also easily broke during the use as they were not stretchable. [12,13] Herein, the EDLC fiber with a coaxial structure had effectively solved the above two critical problems. As shown in Figure 5e,f, the EDLC fiber could be easily bent and woven into various structures with high stability. For instance, the specific capacitances remained almost unchanged after being knotted or woven into textiles (Figure S9, Supporting Information). In addition, the low contacts between two fiber electrodes produced a high internal resistance in the twisted structure, while the coaxial structure has fully taken advantage of the large surface area of CNTs also with a much lower internal resistance. This conclusion has been further verified by comparing the horizontal intercept in the Nyquist plots (Figure 4e) and the voltage spurt part of Galvanostatic charge–discharge curves (Figure 4f). The twisted structure showed much steeper steps than the coaxial structure, so this coaxial EDLC fiber exhibited a much higher specific capacitance of 59 F g^{-1} compared with 4.5 F g^{-1} for the twisted structure.[13]

In summary, novel EDLC fibers in a coaxial structure, to the best of our knowledge, have been firstly realized. The unique

© 2013 WILEY-VCH Verlag GmbH & Co. KGaA, Weinheim

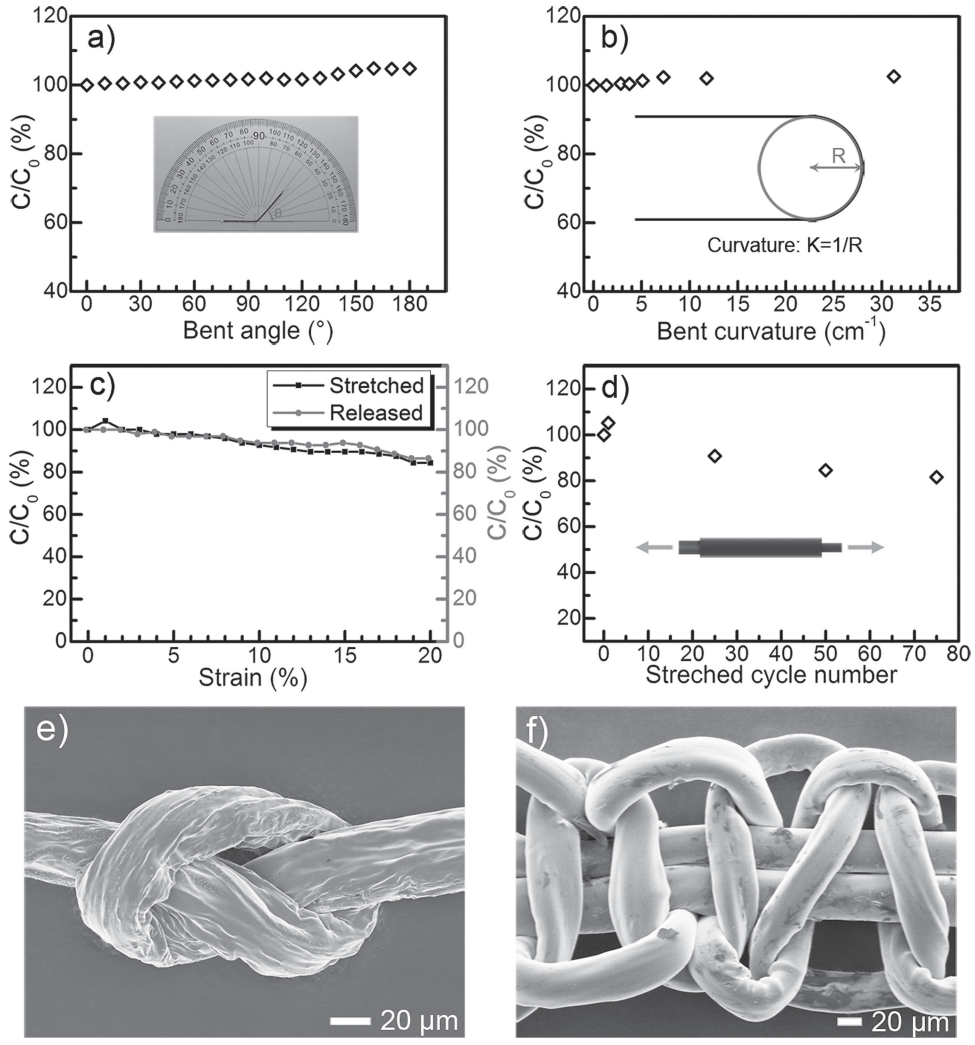

Figure 5. Dependence of specific capacitance on a) bent angle; b) bent curvature; c) strain and d) stretched cycle number (strain of 10%) in the coaxial EDLC fiber. C_0 and C correspond to the specific capacitance before and after bending or stretch, respectively; e) SEM image of a EDLC fiber being made into a knot; f) SEM image of several EDLC fibers being woven into a textile structure.

coaxial structure allows a rapid transportation of ions between the two electrodes with a high electrochemical performance, e.g., a maximum discharge capacitance of 59 F g^{-1} (32.09 F cm^{-3} or 29 μF cm^{-1} or 8.66 mF cm^{-2}), and it has been well maintained at high currents. These EDLC fibers also represent the first demonstration of stretchable energy devices in a fiber format, which is critically important for the practical application in the flexible equipment such as various electronic textiles. This work further provides a general and effective strategy in the development of highly efficient electronic devices.

Experimental Section

The two electrodes, CNT fiber and sheet, were dry-spun from CNT arrays which had been synthesized by chemical vapor deposition.[27] The experimental details are described in the Supporting Information. The gel electrolyte containing PVA and H_3PO_4 was prepared by dissolving 1 g of PVA in 9 g of distilled water at 90 °C for 2 h, followed by cooling down to room temperature and addition of 1 g of H_3PO_4 aqueous solution (85 wt%). The specific capacitances were calculated based on the active materials. The structures were characterized by SEM (Hitachi, FE-SEM S-4800 operated at 1 kV). Galvanostatic charge–discharge characterizations were carried out by an Arbin multi-channel electrochemical testing system (Arbin, MSTAT-5 V/10 mA/16 Ch). Cyclic voltammograms and EIS curves were obtained from an electrochemical analyzer system (CHI 660D). The EIS measurement was made at a potential of 0.1 V in the frequency range of 100 mHz to 1 MHz. For the stretching characterization, the two ends of a EDLC fiber were stabilized on a sample hold, and the stretching process was monitored by an HY0350 Table-top Universal Testing Instrument.

Supporting Information

Supporting Information is available from the Wiley Online Library or from the author.

© 2013 WILEY-VCH Verlag GmbH & Co. KGaA, Weinheim

Acknowledgements

This work was supported by NSFC (91027025, 21225417), MOST (2011CB932503, 2011DFA51330), STCSM (11520701400, 12nm0503200), Fok Ying Tong Education Foundation, Innovative Student Program at Fudan University (EZH2203302/002), and the Program for Professor of Special Appointment at Shanghai Institutions of Higher Learning.

Received: April 5, 2013
Revised: July 8, 2013
Published online: August 16, 2013

[1] M. Kaempgen, C. K. Chan, J. Ma, Y. Cui, G. Gruner, *Nano Lett.* **2009**, *9*, 1872.
[2] M. C. McAlpine, H. Ahmad, D. Wang, J. R. Heath, *Nat. Mater.* **2007**, *6*, 379.
[3] X. Yan, Z. Tai, J. Chen, Q. Xue, *Nanoscale* **2011**, *3*, 212.
[4] C. Meng, C. Liu, S. Fan, *Electrochem. Commun.* **2009**, *11*, 186.
[5] A. G. Pandolfo, A. F. Hollenkamp, *J. Power Sources* **2006**, *157*, 11.
[6] S.-L. Chou, J.-Z. Wang, S.-Y. Chew, H.-K. Liu, S.-X. Dou, *Electrochem. Commun.* **2008**, *10*, 1724.
[7] D. Pech, M. Brunet, H. Durou, P. Huang, V. Mochalin, Y. Gogotsi, P.-L. Taberna, P. Simon, *Nat. Nanotechnol.* **2010**, *5*, 651.
[8] Z. Niu, P. Luan, Q. Shao, H. Dong, J. Li, J. Chen, D. Zhao, L. Cai, W. Zhou, X. Chen, S. Xie, *Energy Environ. Sci.* **2012**, *5*, 8726.
[9] M. D. Stoller, R. S. Ruoff, *Energy Environ. Sci.* **2010**, *3*, 1294.
[10] D. Zhao, Z. Yang, L. Zhang, X. Feng, Y. Zhang, *Electrochem. Solid-State Lett.* **2011**, *14*, A93.
[11] M.-T. Lee, J.-K. Chang, Y.-T. Hsieh, W.-T. Tsai, *J. Power Sources* **2008**, *185*, 1550.
[12] A. B. Dalton, S. Collins, E. Muñoz, J. M. Razal, V. H. Ebron, J. P. Ferraris, J. N. Coleman, B. G. Kim, R. H. Baughman, *Nature* **2003**, *423*, 703.
[13] Z. Cai, L. Li, J. Ren, L. Qiu, H. Lin, H. Peng, *J. Mater. Chem. A* **2013**, *1*, 258.
[14] T. Chen, L. Qiu, Z. Yang, H. Peng, *Chem. Soc. Rev.* **2013**, *42*, 5031.
[15] J. Ren, L. Li, C. Chen, X. Chen, Z. Cai, L. Qiu, Y. Wang, X. Zhu, H. Peng, *Adv. Mater.* **2013**, *25*, 1155.
[16] G. Lota, K. Fic, E. Frackowiak, *Energy Environ. Sci.* **2011**, *4*, 1592.
[17] Y. Jiang, L. Lin, *Sens. Actuators, A* **2012**, *188*, 261.
[18] H.-J. Ahn, J. I. Sohn, Y.-S. Kim, H.-S. Shim, W. B. Kim, T.-Y. Seong, *Electrochem. Commun.* **2006**, *8*, 513.
[19] D. N. Futaba, K. Hata, T. Yamada, T. Hiraoka, Y. Hayamizu, Y. Kakudate, O. Tanaike, H. Hatori, M. Yumura, S. Iijima, *Nat. Mater.* **2006**, *5*, 987.
[20] R. S. Hastak, P. Sivaraman, D. D. Potphode, K. Shashidhara, A. B. Samui, *J. Solid State Electrochem.* **2012**, *16*, 3215.
[21] Y. J. Kang, H. Chung, C.-H. Han, W. Kim, *Nanotechnology* **2012**, *23*, 065401.
[22] X. Sun, T. Chen, Z. Yang, H. Peng, *Acc. Chem. Res.* **2012**, *46*, 539.
[23] L. Liu, A. H. Barber, S. Nuriel, H. D. Wagner, *Adv. Funct. Mater.* **2005**, *15*, 975.
[24] V. Sa, K. G. Kornev, *Carbon* **2011**, *49*, 1859.
[25] J. Lin, C. Zhang, Z. Yan, Y. Zhu, Z. Peng, R. H. Hauge, D. Natelson, J. M. Tour, *Nano Lett.* **2013**, *13*, 72.
[26] B. Vigolo, A. Pénicaud, C. Coulon, C. Sauder, R. Pailler, C. Journet, P. Bernier, P. Poulin, *Science* **2000**, *290*, 1331.
[27] a) H. Peng, X. Sun, F. Cai, X. Chen, Y. Zhu, G. Liao, D. Chen, Q. Li, Y. Lu, Y. Zhu, Q. Jia, *Nat. Nanotechnol.* **2009**, *4*, 738; b) Z. Yang, T. Chen, R. He, G. Guan, H. Li, L. Qiu, H. Peng, *Adv. Mater.* **2011**, *23*, 5636.

© 2013 WILEY-VCH Verlag GmbH & Co. KGaA, Weinheim